Relevance of brain lesion location for cognition in vascular mild cognitive impairment

Antonio Giorgio[a,*], Ilaria Di Donato[a], Alessandro De Leucio[a], Jian Zhang[a], Emilia Salvadori[b], Anna Poggesi[b], Stefano Diciotti[c], Mirco Cosottini[d], Stefano Ciulli[e], Domenico Inzitari[b], Leonardo Pantoni[f], Mario Mascalchi[e], Antonio Federico[a], Maria Teresa Dotti[a], Nicola De Stefano[a], on behalf of the VMCI-Tuscany Study Group[1]

[a] Department of Medicine, Surgery and Neuroscience, University of Siena, Siena, Italy
[b] NEUROFARBA Department, Neuroscience Section, University of Florence, Florence, Italy
[c] Department of Electrical, Electronic, and Information Engineering "Guglielmo Marconi", University of Bologna, Cesena, Italy
[d] Department of Translational Research and New Technologies in Medicine and Surgery, University of Pisa, Pisa, Italy
[e] Department of Clinical and Experimental Biomedical Sciences -"Mario Serio", University of Florence, Florence, Italy
[f] "L. Sacco" Department of Biomedical and Clinical Sciences, University of Milano, Italy

ARTICLE INFO

ABSTRACT

Background: Vascular mild cognitive impairment (VMCI) is a potentially transitional state between normal aging and vascular dementia. The presence of macroscopic white matter lesions (WML) of moderate or severe extension on brain MRI is the hallmark of the VMCI.

Objective: To assess the clinical relevance of the frequency of WML in patients with VMCI independently of total lesion volume (LV).

Methods: In this multicenter study, we included 110 patients with VMCI (age: 74.3 ± 6.6 years; sex: 60 women). Cognitive assessment was performed with the VMCI-Tuscany Neuropsychological Battery, which allowed to identify four VMCI groups: amnestic single ($n = 9$) and multi-domain ($n = 76$), non-amnestic single- ($n = 10$) and multi-domain ($n = 15$). Distribution and frequency of WML on MRI FLAIR images were evaluated with lesion probability map (LPM). Voxelwise statistics was performed with nonparametric permutation tests, controlling for age, sex, slice thickness, center, magnetic field strength, total LV and head size ($p < .01$, family-wise error-corrected for multiple comparisons across space).

Results: LPM of the WML had a fairly symmetric and widespread distribution across brain. A higher frequency of WML along association tracts of the WM such as inferior longitudinal fascicle, inferior fronto-occipital fascicle and superior longitudinal fascicle, was correlated with worst cognitive scores at the Trail Making Test Part A and

* Corresponding author at: Quantitative Neuroimaging Laboratory, Department of Medicine, Surgery and Neuroscience, University of Siena, Viale Bracci 2, 53100 Siena, Italy.
E-mail addresses: giorgio3@unisi.it (A. Giorgio), emilia.salvadori@unifi.it (E. Salvadori), anna.poggesi@unifi.it (A. Poggesi), stefano.diciotti@unibo.it (S. Diciotti), domenico.inzitari@unifi.it (D. Inzitari), leonardo.pantoni@unimi.it (L. Pantoni), mario.mascalchi@unifi.it (M. Mascalchi), federico@unisi.it (A. Federico), dotti@unisi.it (M.T. Dotti), destefano@unisi.it (N. De Stefano).

Copy of the Rey–Osterrieth Complex Figure. The non-amnestic groups showed a higher frequency of WML in the anterior cingulum and superior longitudinal fascicle close to the frontal gyrus.

Conclusions: Our study showed that in patients with VMCI, independently of total LV, the higher frequency of lesions along association tracts of the WM, which mediate intrahemispheric long-range connectivity, is related with psychomotor speed and constructional praxis. Moreover, a prevalence of lesions in the frontal WM seems to characterize VMCI patients with involvement of non-amnestic domains.

1. Introduction

White matter lesions (WML) visible on MRI scans of elderly subjects were traditionally disregarded as anticipated effect of normal aging. However, recent studies suggest that WML may represent the diagnostic hallmark of mild cognitive impairment (MCI) due to small vessel disease (SVD), the so-called vascular MCI (VMCI), a term defining a potentially transitional state between normal aging and vascular dementia (O'Brien et al., 2003). Indeed, a large meta-analysis of longitudinal studies has recently shown that in elderly subjects WML are linked with cognitive decline and carry a risk of subsequent dementia and stroke (Debette and Markus, 2010).

The neuropathological substrates of WML in VMCI are heterogeneous, consisting of local demyelination from oligodendrocytes apoptosis, axonal loss, astrogliosis and arteriolar fibrohyalinosis, and the pathogenic mechanisms of WML formation in this context are also incompletely understood, being mainly represented by ischemic damage and partly by microglia activation and increased water content from blood-brain barrier dysfunction (Wardlaw et al., 2015). However, the potential clinical relevance of the VMCI is likely higher than that of degenerative MCI, given that management of risk factors and pharmacological treatment can prevent the evolution to vascular dementia (Pantoni, 2010).

Although the association between WML load and cognition in aging and SVD has been traditionally recognized (Kuo and Lipsitz, 2004; Pantoni et al., 2007), the relevance of WML location and microstructural tissue damage outside them has been generally underestimated. As for the first aspect, early evidence came from small case series of patients with acute infarcts in specific subcortical structures (e.g., thalamus, anterior limb of the internal capsule, corpus callosum) (Biesbroek et al., 2017). Although a number of studies provided conflicting or negative results, the periventricular but not subcortical group of the WML, considered as a whole, were found by a systematic review to be correlated in older adults with the executive function and processing speed (Bolandzadeh et al., 2012) and linked, in a 10-year longitudinal study, with a faster general cognitive decline over time (De Groot et al., 2002). In terms of the damage to normal-appearing WM in VMCI, which was recognized for the first time a few years ago with the application of diffusion tensor imaging (DTI) (Maillard et al., 2011), a recent DTI work from our study group highlighted its contribution for the global cognitive performance of these patients (Mascalchi et al., 2018).

Despite these previous studies, it is still currently unknown whether in the VMCI the spatial distribution and frequency of WML in particular brain locations, and not just in large regions, may lead to a "strategic" damage of the WM tracts critical for cognition. To test such hypothesis, we used the MRI-derived lesion probability map (LPM), a powerful location-based image analysis approach that is able to assess at group level the clinical relevance of WML and that has been previously applied to several WM disorders (Enzinger et al., 2006; DeCarli et al., 2005; Giorgio et al., 2013; Matthews et al., 2013; Narayanan et al., 1997; Wen and Sachdev, 2004). By avoiding the biases of predefined regions of interest and of the WML grouping based on large regions and taking into account the complexity of brain anatomy, LPM evaluates in vivo the anatomical distribution and frequency across all brain lesions, thus allowing to capture the spatial patterns of focal pathology that could not be evident in a single-patient evaluation.

2. Materials and methods

2.1. Study subjects

In this multicenter study, we assessed 110 patients with VMCI (age: 74.3 ± 6.6 years; sex: 60 women, 50 men) characterized by WML of moderate ($n = 52$) or severe ($n = 58$) extension who were enrolled at the University Hospitals of Florence, Pisa and Siena in the context of the VMCI-Tuscany study (Poggesi et al., 2012).

Inclusion criteria were: 1) clinical diagnosis of MCI according to the Winblad criteria (Winblad et al., 2004), recently operationalized (Salvadori et al., 2016), and 2) MRI evidence on FLAIR/T2-weighted images of moderate or severe degree of WML, according to the modified version of the Fazekas scale (Pantoni et al., 2005). Exclusion criteria were: presence of other conditions with WML, inability to provide an informed consent, presence of non-lacunar infarcts in the GM or hemorrhagic lesions, whose tissue damage may be a confounder in the interpretation of ischemic WML mapping.

Enrolled patients underwent a complete neuropsychological and MRI examination.

2.2. Standard protocol approvals, registrations, and patient consents

The study was performed in accordance with the Helsinki Declaration and approved by local ethics boards. A written informed consent was obtained from all study participants.

2.3. Neuropsychological assessment

VMCI-Tuscany Neuropsychological Battery (Salvadori et al., 2015) is based on 14 tests, with corresponding age- and education-adjusted scores. In detail, it comprises two tests of global mental functioning such as Mini Mental State Examination (MMSE) and Montreal Cognitive Assessment Battery (MoCA).

The battery also includes 12 domain-specific or second-level tests, targeting a wide range of cognitive abilities: four tests for memory (Rey Auditory-Verbal Learning Test [RAVL] immediate and delayed recall and Short Story for verbal memory; Rey–Osterrieth Complex Figure [ROCF] recall for visuo-spatial memory), five tests for attention and executive functions (Trail Making Test [TMT] Part A for psychomotor speed; Visual Search [number of matrices] for focused attention; Symbol Digit Modalities Test [SDMT] for sustained attention; Color Word Stroop Test for selective attention; TMT Part B for divided attention), two tests for language (Phonemic and Semantic Verbal Fluency) and one test for constructional praxis (ROCF copy).

Cognitive scores were available in all patients for all tests and in 47 patients for TMT Part A and B, due to the time limit of their administration procedure, so that if a patient does not complete the task within 5 min, the examiner stops the test administration and scores are not obtained.

2.4. MRI data acquisition and analysis

MRI data were acquired on scanners operating at 1.5T ($n = 94$) and 3T ($n = 19$).

For the purpose of this study, we assessed high-resolution 3D (1mm^3) T1-weighted (T1-W) images and FLAIR images (slice thickness:

3 mm [$n = 16$], 3.6 mm [$n = 75$], 5 mm [$n = 19$]).

All MRI data were sent to the Quantitative Neuroimaging Laboratory (QNL) of the University of Siena for quality control and centralized MRI analysis.

WML were outlined on FLAIR images by using a semiautomated segmentation technique based on user-supervised local thresholding (Jim; www.xinapse.com/Manual/). Total lesion volume (LV) was computed by multiplying lesion area by slice thickness.

A FLAIR-lesion probability map (LPM) of WML in the whole VMCI study sample was created using tools of the FMRIB Software Library (FSL, www.fmrib.ox.ac.uk/fsl/ (Smith et al., 2004; Jenkinson et al., 2012)).

First, a symmetric (i.e., with the same number of age-matched patients from each center) study-specific template in standard space was obtained after registering a sample ($n = 48$) of 3D T1-W images onto the high-resolution (1mm^3) MNI152 standard brain image by using first linear (FLIRT [FMRIB Linear Image Registration Tool], 6 degrees of freedom [DOF]) (Jenkinson and Smith, 2001), then refinement with

Table 1
Demographic, clinical and MRI characteristics of the whole VMCI patient study sample and of the four cognitive phenotypes.

	Whole VMCI sample (n = 110)	Amnestic/single-domain ASD (n = 9)	Amnesti/multi-domain AMD (n = 76)	Non-amnestic/single-domain NASD (n = 10)	Non-amnestic/multi-domain NAMD (n = 15)	p-Value (group comparisons)
Age, years	74.3 ± 6.6	74.2 ± 6.5	74.4 ± 6.7	72 ± 7.2	75.5 ± 6.2	0.63
Sex (male/female)	60/50	7/2	39/37	6/4	8/7	0.48
Education, years	8.3 ± 4.2	7.8 ± 3.3	8.4 ± 4.4	8.9 ± 4.5	7.6 ± 4.05	0.85
Vascular risk factors						
Hypertension (y/n)	87/23	4/5	64/12	7/3	12/3	0.04
Hypercholesterolemia (y/n)	66/44	6/3	45/31	6/4	9/6	0.98
Hypertrigliceridemia (y/n)	25/85	1/8	17/59	4/6	3/12	0.48
Diabetes (y/n)	17/93	0/9	17/59	0/10	0/15	0.03
Smoking (y/n)	52/58	4/5	34/42	6/4	8/7	0.77
History of stroke (y/n)	33/77	3/6	21/55	5/5	4/11	0.52
Alcohol consumption (y/n)	33/77	3/6	22/54	1/9	7/8	0.26
Physical activity (y/n)	30/80	3/6	20/56	4/6	3/12	0.70
Global cognition						
MMSE (range 0–30)*	27.2 ± 2.7	27.8 ± 2.2	27.1 ± 2.8	27.2 ± 2.8	27.5 ± 2.8	0.86
MoCA (range 0–30)*	21.2 ± 4.4	21 ± 2.1	21.4 ± 4.6	20 ± 4.4	21.3 ± 4.2	0.85
Memory						
RAVL immediate recall (range 0–75)*	32.4 ± 8.6	35.5 ± 6.6	32.2 ± 8.7	30.5 ± 7.5	32.9 ± 10.4	0.63
RAVL delayed recall (range 0–15)*	6.1 ± 2.8	6.8 ± 2.7	6 ± 2.9	6 ± 1.9	6.2 ± 3	0.90
Short Story (range 0–28)*	11.7 ± 4.1	10.8 ± 3	11.8 ± 4	10.7 ± 3.9	12.4 ± 5.5	0.70
ROCF recall (range 0–36)*	12 ± 5.6	12.5 ± 3.7	12.3 ± 6	9.6 ± 3.7	11.6 ± 4.7	0.58
Attention and executive functions						
TMT-A (time to complete, secs)**	67.3 ± 50.1	62.3 ± 32	67.2 ± 53.9	81.4 ± 45.5	63.5 ± 44.8	0.85
Visual Search (range 0–50)*	31.8 ± 9	40.3 ± 5.6	30.3 ± 8.8	33.4 ± 12.8	32.8 ± 5.4	0.01 (AMD < ASD, p = .008)
SDMT (correct answers in 90 s)*	34.4 ± 10.4	33.3 ± 6.3	34.8 ± 10.4	30 ± 8.7	35.4 ± 13.5	0.56
Stroop test (time to complete, secs)**	36.6 ± 31.2	17.3 ± 7	40.2 ± 35	25.2 ± 11	37 ± 23.3	0.12
TMT-B (time to complete, secs)**	104.4 ± 60	114.8 ± 71	104.4 ± 60	121 ± 82.3	88.3 ± 41	0.84
Language						
Phonemic verbal fluency (words in 3 mins)*	28.1 ± 9.6	35.5 ± 9.3	26.4 ± 9.4	35 ± 7.6	27.8 ± 8.16	0.004 (ASD > AMD, p = .0028; NASD > AMD, p = .029)
Semantic verbal fluency (words in 3 mins)*	34.3 ± 7.7	38.3 ± 6.1	33 ± 8	39 ± 6.6	35 ± 6.4	0.03 (no sign. at post-hoc analysis)
Constructional praxis						
ROCF copy (range 0–36)*	23.8 ± 9.1	26.7 ± 4.5	23.7 ± 9.3	19 ± 12.4	25.1 ± 7.6	0.28
MRI source						
Centers						0.24
1	75	7	55	3	10	
2	19	1	11	4	3	
3	16	1	10	3	2	
Field strength						0.22
1.5 T	91	8	65	6	12	
3.0 T	19	1	11	4	3	
LV (median [interquartile range]),^ cm³	25.3 [15.9–39 cm³]	19 [15.7–32.3 cm³]	25.3 [16.2–38.8 cm³]	26.4 [20.7–32.3 cm³]	31.49 [14.5–59 cm³]	0.87

All cognitive test were corrected by age and education.
* Higher scores correspond to better performance.
** Lower scores correspond to a better performance.
^ in native space.

nonlinear registration (FNIRT [FMRIB Nonlinear Image Registration Tool]) (Andersson et al., n.d.) and, finally, by merging and averaging all the registered images.

Second, WML mask of each patient was nonlinearly registered onto the template with the tool "applywarp" (nearest neighbour interpolation) using both the linear matrix obtained from registration of FLAIR onto the T1-W image with FLIRT ("boundary-based registration" cost function, 6 DOF) and the warp field coefficient obtained from registration of T1-W image onto the template with FLIRT and then FNIRT. Two experienced observers (AG and ADL) independently checked all the registered WML masks onto the template and an agreement was found in all cases.

Finally, LPM was generated first merging and then averaging all the FLAIR-lesion masks previously registered onto the template.

2.5. Statistical analysis

2.5.1. General statistics

Differences among the four VMCI groups were tested with Chi-Square for sex, vascular risk factors, MRI source (center, magnetic field strength) and analysis of variance (ANOVA) for age, education, cognitive tests and total LV, which was log-transformed in order to obtain a normal distribution.

Correlations between total LV and cognitive scores were assessed with Spearman coefficient.

Significance was set at $p < .05$. SPSS (IBM, www.ibm.com) was used to perform all calculations.

2.5.2. Voxelwise statistics

All analyses were performed with *randomise*, a nonparametric permutation ($n = 5000$ permutations) FSL program. Designs (matrices and contrasts) were created in the voxelwise general linear model framework. In particular, we used correlation analyses between voxelwise WML frequency (as independent variable) and the different cognitive tests (as dependent variable). In addition, we used unpaired *t*-tests for two-group comparisons (i.e., non-amnestic vs amnestic groups as a whole, single-domain vs multi-domain groups as a whole) and ANOVA

(F-test followed by post-hoc pairwise unpaired *t*-tests) for four-group comparisons (i.e., among the VMCI cognitive groups).

In all the analyses, we controlled for age, sex, FLAIR slice thickness, center, magnetic field strength, total LV (in native space) and head size (assessed with the normalized scaling factor derived from SIENAX (Smith et al., 2002)). Thresholding was performed using TFCE (Threshold-Free Cluster Enhancement) (Smith and Nichols, 2009). All the analyses were corrected for multiple comparisons across space using the Family-Wise Error method with $p < .01$, given the number of analyses performed ($n = 28$ correlations and $n = 12$ comparisons) and the explorative nature of the study.

Voxelwise correlation coefficients were obtained computing Pearson correlation coefficient between frequency of WML averaged across significant clusters and corresponding cognitive test score.

Anatomical location of the local maxima within significant clusters was determined using the Johns Hopkins University (JHU) DTI-based WM atlases implemented in FSL (i.e., ICBM-DTI-81 white-matter labels atlas and JHU white-matter tractography atlas).

3. Results

3.1. Whole VMCI study sample and cognitive groups

Table 1 reports demographic, clinical and MRI characteristics of the whole VMCI patient population ($n = 110$) and the four cognitive groups, identified according to the involvement of cognitive domains using the classification strategy of the VMCI-Tuscany Neuropsychological Battery: amnestic/single-domain (ASD, $n = 9$), amnestic/multi-domain (AMD, $n = 76$), non-amnestic/single-domain (NASD, $n = 10$), non-amnestic/multi-domain (NAMD, $n = 15$) (Table 1).

3.2. WML spatial distribution

In the whole VMCI study sample, median total LV (computed on FLAIR images) was 25.3 cm^3 (interquartile range: 15.9–39 cm^3).

MRI-derived LPM (Fig. 1) had a fairly symmetric and widespread distribution across brain, with a particularly high WML frequency
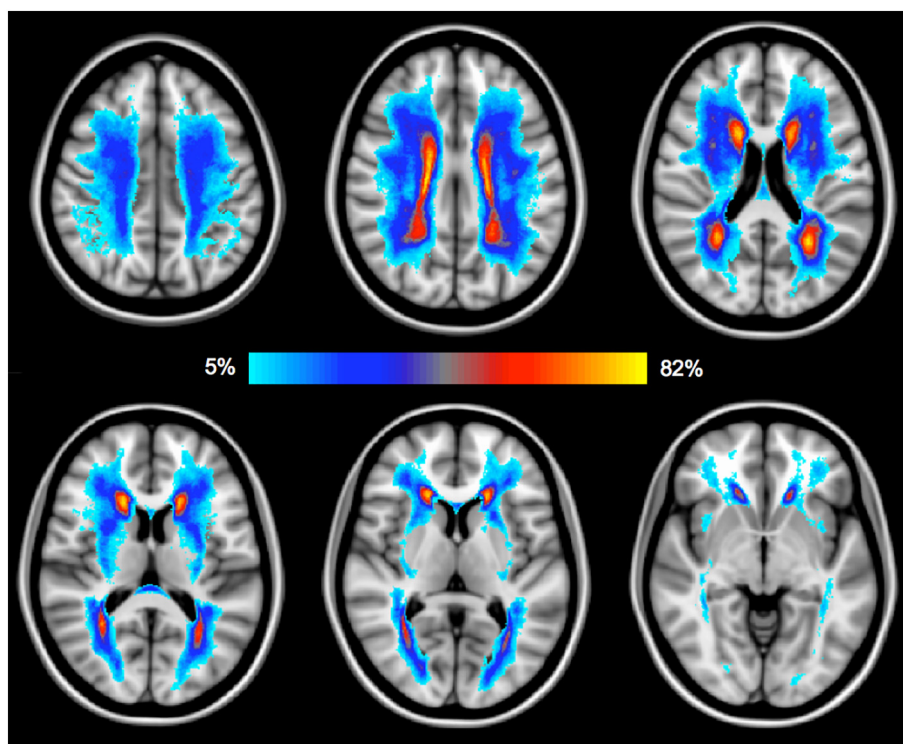
Fig. 1. Lesion probability map (LPM) in our sample of VMCI patients is shown. The color overlay created on top of the MNI152 standard brain represents the probability of WML occurrence, with the light-blu to yellow color range representing the frequency of lesions in specific anatomical locations. Lower slices (i.e., brainstem, cerebellum) are not shown due to the presence of very few WML. Images are shown in radiological orientation (i.e., right side is left hemisphere). (For interpretation of the references to color in this figure legend, the reader is referred to the web version of this article.)

around the anterior and posterior horns of the lateral ventricles and in the centrum semiovale.

3.3. Correlations between cognitive tests and WML frequency

In terms of general statistics, significant ($p \leq .02$) but weak (r values from 0.22 to 0.28) correlations were only found between total LV and MoCA, TMT-A, ROCF (copy and recall) and RAVL immediate (Table 2).

However, at the whole-brain voxelwise analysis we found correlations ($p < .01$, corrected) between higher WML frequency in specific locations and two of the 14 cognitive tests. Indeed, higher TMT-A scores (i.e., lower psychomotor speed) correlated ($r = 0.65$, $p < .001$) with higher frequency of WML in the inferior longitudinal fascicle (ILF), inferior fronto-occipital fascicle (IFOF) and SLF close to angular gyrus (AG) and superior parietal lobule (SPL). Moreover, lower scores of the Copy of ROCF (i.e., lower constructional praxis) correlated ($r = -0.63$, $p < .001$) with higher WML frequency in the IFOF.

(Table 3, Fig. 2)

Given that the AMD represented the largest cognitive group, we also restricted to it the correlation analysis between cognitive tests and frequency of the WML. However, no significant clusters were found.

3.4. Comparison of WML frequency among VMCI cognitive groups

The non-amnestic (NA) groups (i.e., NASD and NAMD) showed higher ($p < .01$, corrected) WML frequency than amnestic (A) group (i.e., ASD and AMD) in the anterior cingulum (Cg) (Fig. 3). By contrast, no differences were found between single-domain (ASD and NASD) and multi-domain (AMD and NAMD) groups.

The four VMCI cognitive groups showed heterogeneity in the frequency of WML ($p < .01$, corrected). In particular (Table 4, Fig. 3), this was higher in NAMD than NASD in the SLF adjacent to the inferior frontal gyrus (IFG), in NAMD than AMD in the anterior Cg and in the SLF adjacent to the middle frontal gyrus (MFG).

4. Discussion

Given the negative impact on daily activities of the cognitive impairment in the VMCI and the potential to prevent its evolution to dementia, it becomes crucial understanding at group level first whether and to what extent topography of the macroscopic pathology of the WM, in terms of frequency of WML in specific locations, might help elucidate disease mechanisms. To provide an answer to this unclear issue, we performed voxelwise analyses across the whole lesional area in a relatively large sample of VMCI patients, without any a priori knowledge that could potentially bias the results. We found that, independently of total LV i) a higher frequency of WML along specific association tracts of the WM is closely related to specific patterns of cognitive impairment, and ii) different cognitive groups can have a different WML topography.

4.1. Association between topography of WML and cognition in the whole VMCI study sample

We did not find significant voxelwise correlations between frequency of WML and tests of global cognition such as MMSE and MoCA.

Among the various domain-specific cognitive tests, those showing significant correlation with a higher frequency of WML in specific regions, independently of total LV, were TMT-A and Copy of ROCF. In particular, higher scores of TMT-A, reflecting lower psychomotor speed, were associated with a higher frequency of WML in the parieto-occipital lobe, mainly mapping on ILF, IFOF and SLF adjacent to the AG and SPL.

Moreover, lower scores of the Copy of ROCF, representing lower constructional praxis, showed association with WM regions of the IFOF.

The exact mechanisms underpinning the impact of the topography of WML on the cognition of VMCI patients are still incompletely

understood and might not depend on the direct effect of WML. Results of the present study depict a significant clinical role for WML along association tracts (e.g., ILF, IFOF, SLF). A plausible mechanism would be the preferential disruption of this type of WM fibers, known to mediate intrahemispheric long-range connectivity.

4.2. Topography of WML and VMCI cognitive groups

Among the four cognitive groups of VMCI, topography of WML showed significant results despite the absence of group heterogeneity in the overall WML load. In particular, a prevalence of WML along the association tracts of the frontal lobe (SLF and cingulum) characterized the patients with the non-amnestic type of cognitive impairment. This finding stresses once again the clinical relevance of the preferential involvement of the association tracts of the WM in VMCI. Moreover, the higher frequency of WML in the frontal lobe of patients with non-amnestic VMCI, especially of the multi-domain type, may represent an early sign of a possible future development of dementia, in line with the "retrogenesis" (i.e., reverse to myelin development) model of the WM degeneration occurring first in the late-myelinating and small-diameter fibers of the anterior WM (Alves et al., 2015; Vik et al., 2015; Brickman et al., 2012). In support of this, nonamnestic VMCI has indeed been proposed, especially in presence of high WML load (Devine et al., 2013), as prodromal stage of vascular dementia (Seo et al., 2010; Frisoni et al., 2002).

In pathogenic terms, it is plausible that higher frequency of frontal WML along association tracts may lead to a disconnection of the fronto-subcortical circuitry, which connects structures of the deep GM with corresponding regions of the frontal cortex such as dorsolateral prefrontal, anterior cingulate and orbitofrontal circuits.

4.3. Study strengths and limitations

In general, a voxel-based study such as that performed here has strengths and limitations. Strength lies in the ability to study a relatively large population of patients with VMCI and provide clinically relevant pieces of information, which would be hard to achieve with a simple visual assessment of WML in single patients. Some methodological aspects are also worthy of mention: the use of nonlinear registration for creation of the LPM allows alignment of patients' brains with great accuracy, diminishing potential registration errors; voxelwise analyses were based on the nonparametric permutation test, which is applicable even when the assumptions of a parametric approach are not valid, as in the case of study groups with very different numbers of subjects; the use of correction for multiple comparisons across space and a conservative cluster-forming threshold for all voxelwise analyses, thus reducing the risk of false-positive results; finally, the correction of all our analyses for total LV allowed us to determine that results were specific to a particular anatomic area and independent of the total WML load, and as such valid in patients with low and high total LV.

Our study is not without limitations. First, MRI data from the three centers were acquired with different sequence geometry and field strength. While limited evidence exists in VMCI on a direct comparison of WML at different magnetic field strengths (Wardlaw et al., 2015),

Table 2

Significant correlations between total LV and cognitive scores in the whole VMCI study sample.

| Cognitive test	Rho coefficient	p-value
MOCA	−0.24	0.014
RAVL immediate	−0.22	0.02
ROCF (recall)	−0.27	0.006
TMT-A	0.25	0.012
ROCF (copy)	−0.28	0.02

See text for abbreviations.

Table 3
WM regions where a higher frequency of WML was associated with worst scores of cognitive tests in our sample of VMCI patients ($p < .01$, corrected for multiple comparisons across space). Correlation analyses were controlled for age, sex, FLAIR slice thickness, center, magnetic field strength, total LV (in native space) and head size.

Test (cognitive domain)	WM tract	Type of WM tract	Lobe	Side	MNI X,Y,Z (mm)*	Cluster size (voxel count)	P-value
TMT-A (psychomotor speed)	ILF	Association	Occipital	R	36, −62, 9	1110	< 0.001
	IFOF	Association	Occipital	R	25,-92,4	326	0.003
	SLF (angular gyrus)	Association	Occipital	L	−40,-61,21	262	0.006
	SLF (superior parietal lobule)	Association	Parietal	L	−24,-50,59	148	0.007
	ILF	Association	Occipital	L	−25,-70,20	104	0.005
	ILF	Association	Occipital	L	−37,-63,9	57	0.006
	SLF (angular gyrus)	Association	Parietal	R	50,-53,36	45	0.006
ROCF-copy (constructional praxis)	IFOF	Association	Temporal	L	−35,-51,-2	28	0.009
	IFOF	Association	Temporal	L	−38,-39,-4	12	0.009

* Local maxima of significant cluster.
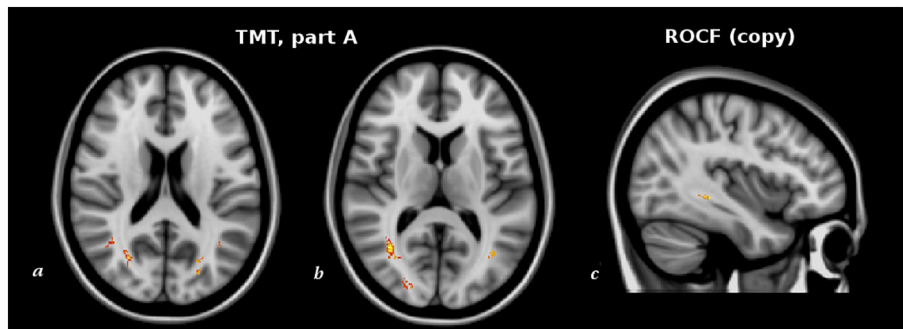
Fig. 2. Red-yellow shows the clusters of voxels where a higher frequency of WML was associated ($p < .01$, corrected fro multiple comparisons across space) with worst cognitive scores at the TMT part A (a, b) and ROCF (copy) (c) in our sample of patients with VMCI. Correlation analyses were controlled for age, sex, FLAIR slice thickness, center, magnetic field strength, total LV (in native space) and head size. The most informative slices are shown. Background image is MNI152 standard brain, in radiological orientation (i.e., right side is left hemisphere).
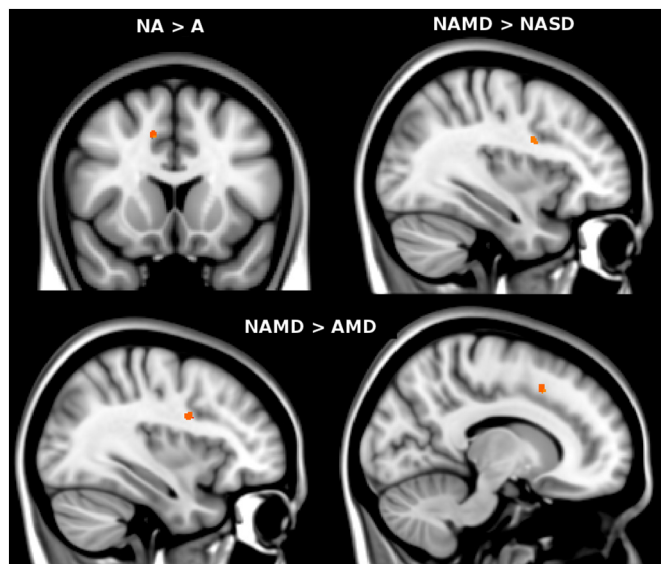
Fig. 3. Red-yellow shows the clusters of voxels where a higher frequency of WML ($p < .01$, corrected fro multiple comparisons across space) was present in non-amnestic (NA) vs amnestic (A) group (upper panel, top left), in non-amnestic multi-domain (NAMD) vs non-amnestic single-domain (NASD) group (upper panel, top right) and in non-amnestic multi-domain (NAMD) vs amnestic multi-domain (AMD) group (lower panel). Comparison analyses were controlled for age, sex, FLAIR slice thickness, center, magnetic field strength, total LV (in native space) and head size. The most informative slices are shown. Background image is MNI152 standard brain, in radiological orientation (i.e., right side is left hemisphere). (For interpretation of the references to color in this figure legend, the reader is referred to the web version of this article.)

recent studies in multiple sclerosis, another neurological condition with WML, demonstrated that 3 T is able to detect 15% more lesions than 1.5 T MRI, although this did not reach significance or influence MS

diagnosis in terms of dissemination of lesions in space and time (Hagens et al., 2018a; Hagens et al., 2018b). Nevertheless, the use of nonlinear registration and correction of all voxelwise analyses for the slice thickness, center and magnetic field strength, as already performed in several previous studies, should have not affected the overall anatomical distribution and frequency of occurrence of WML.

Second, another limitation, which is intrinsic to the design of a cross sectional study, is the assessment of "static" distribution and frequency of the WML, which ideally, provided that longitudinal MRI data are available, should be followed over multiple time-points in order to weigh their prognostic role for a possible conversion of the VMCI to dementia.

Third, the presence of a control group with normal cognition would have furthered our understanding and highlighted the specificity of the spatial patterns of lesions in the VMCI.

Fourth, the lack of biomarkers of neurodegeneration (e.g., cerebrospinal fluid proteins and positron emission tomography) did not allow to definitely establishing the etiology of our condition (i.e., purely vascular or a combined form of MCI). However, we also recognize that this reflects a common situation in clinical practice.

Finally, we selected a homogeneous sample of patients with "pure" ischemic focal WM pathology, excluding those with non-lacunar infarcts in the GM or with hemorrhagic lesions, whose tissue damage might have created problems in the interpretation of the LPM.

4.4. Conclusions

Overall, by exploiting the potential of the MRI-derived LPM, which allows a spatial analysis of the lesions at group level we demonstrated, independently of total lesion load, a variable spatial vulnerability of the WM to focal pathology of ischemic type, probably leading to a "strategic" disconnection along the association tracts of the WM that may explain specific aspects of cognitive impairment in patients with VMCI. Since association tracts of the WM are known to mediate long-range connectivity between distant GM regions of the same hemisphere, this

Table 4
WM regions with differences in lesion frequency among the cognitive groups of VMCI ($p < .01$, corrected): amnestic single-domain (ASD), amnestic multi-domain (AMD), non-amnestic single-domain (NASD) and non-amnestic multi-domain (NAMD). Comparison analyses were controlled for age, sex, FLAIR slice thickness, center, magnetic field strength, total LV (in native space) and head size.

Group comparison	WM tract	Type of WM tract	Lobe	Side	MNI X,Y,Z (mm)[*]	Cluster size (voxel count)	P-value
NA (SD + MD) > A (SD + MD)	Cg	Association	Frontal	R	13,14,43	18	0.001
NAMD > NASD	SLF (IFG)	Association	Frontal	R	31,4,27	23	0.002
NAMD > AMD	Cg	Association	Frontal	R	13,14,43	27	< 0.001
	SLF (MFG)	Association	Frontal	R	38,5,31	24	0.001

[*] Local maxima of significant cluster.

finding is particularly important in highlighting the role of the multi-focal pathology of the WM in VMCI. Indeed, this fits with the early notion of VMCI as a "disconnection syndrome" secondary to the damage of WM affecting the cognitively relevant structures of the GM at the level of interconnecting association tracts of the WM (O'Sullivan et al., 2001; Catani and ffytche, 2005).

The increasing recognition of the cognitive relevance of WML in specific locations with respect to the global assessment of lesion load, also supported by the new methods of multivariate lesion analysis with machine learning algorithms (Karnath et al., 2018), might be useful for the interpretation of MRI examinations of single patients in clinical practice and for the design of tailored clinical interventions at group level.

Acknowledgements

Ethical approval

All procedures performed in studies involving human participants were in accordance with the ethical standards of the institutional and/or national research committee and with the 1964 Helsinki declaration and its later amendments or comparable ethical standards.

Informed consent

Informed consent was obtained from all individual participants included in the study.

Disclosure of conflict of interest

The Authors report no disclosures specific for this study.

Author contribution

Name	Location	Role	Contribution
Antonio Giorgio, MD PhD	University of Siena	Author	Study concept and design, acquisition, analysis and interpretation of data, drafting manuscript
Ilaria Di Donato, MD	University of Siena	Author	Acquisition of data
Alessandro De Leucio, MD	University of Siena	Author	Analysis of data
Jian Zhang, MD	University of Siena	Author	Analysis of data
Emilia Salvadori, PhD	University of Florence	Author	Acquisition of data
Anna Poggesi, MD PhD	University of Florence	Author	Acquisition of data
Stefano Diciotti, PhD	University of Bologna	Author	Interpretation of data, critical revision of manuscript for intellectual content
Mirco Cosottini, MD PhD	University of Pisa	Author	Acquisition of data
Stefano Ciulli, PhD	University of Florence	Author	Acquisition of data
Domenico Inzitari, MD PhD	University of Florence	Author	Critical revision of manuscript for intellectual content
Leonardo Pantoni, MD PhD	University of Milano	Author	Critical revision of manuscript for intellectual content
Mario Mascalchi, MD PhD	University of Florence	Author	Critical revision of manuscript for intellectual content
Antonio Federico, MD PhD	University of Siena	Author	Critical revision of manuscript for intellectual content
Maria Teresa Dotti, MD PhD	University of Siena	Author	Study concept and design, critical revision of manuscript for intellectual content
Nicola De Stefano, MD PhD	University of Siena	Author	Study concept and design, interpretation of data, critical revision of manuscript for intellectual content

References

Alves, G.S., Oertel Knochel, V., Knochel, C., et al., 2015. Integrating retrogenesis theory to Alzheimer's disease pathology: insight from DTI-TBSS investigation of the white matter microstructural integrity. Biomed. Res. Int. 2015, 291658.

Andersson JLR, Jenkinson M, Smith S. Non-linear Registration, Aka Spatial Normalisation. FMRIB Technical Report TR07JA2 from Wwwfmriboxacuk/Analysis/Techrep 2007:1–21.

Biesbroek, J.M., Weaver, N.A., Biessels, G.J., 2017 Apr 25. Lesion location and cognitive impact of cerebral small vessel disease. Clin. Sci. (Lond.) 131 (8), 715–728.

Bolandzadeh, N., Davis, J.C., Tam, R., Handy, T.C., Liu-Ambrose, T., 2012 Oct 30. The association between cognitive function and white matter lesion location in older adults: a systematic review. BMC Neurol. 12, 126.

Brickman, A.M., Meier, I.B., Korgaonkar, M.S., et al., 2012 Aug. Testing the white matter retrogenesis hypothesis of cognitive aging. Neurobiol. Aging 33 (8), 1699–1715.

Catani M, ffytche DH. The rises and falls of disconnection syndromes. Brain 2005 Oct;128(Pt 10):2224–39.

De Groot, J.C., De Leeuw, F.E., Oudkerk, M., et al., 2002 Sep. Periventricular cerebral white matter lesions predict rate of cognitive decline. Ann. Neurol. 52 (3), 335–341.

Debette, S., Markus, H.S., 2010 Jul 26. The clinical importance of white matter hyperintensities on brain magnetic resonance imaging: systematic review and meta-analysis. BMJ 341, c3666.

DeCarli, C., Fletcher, E., Ramey, V., Harvey, D., Jagust, W.J., 2005 Jan. Anatomical mapping of white matter hyperintensities (WMH): exploring the relationships between periventricular WMH, deep WMH, and total WMH burden. Stroke 36 (1), 50–55.

Devine, M.E., Fonseca, J.A., Walker, Z., 2013 Jan. Do cerebral white matter lesions influence the rate of progression from mild cognitive impairment to dementia? Int. Psychogeriatr. 25 (1), 120–127.

Enzinger, C., Smith, S., Fazekas, F., et al., 2006 Aug. Lesion probability maps of white matter hyperintensities in elderly individuals: results of the Austrian stroke prevention study. J. Neurol. 253 (8), 1064–1070.

Frisoni, G.B., Galluzzi, S., Bresciani, L., Zanetti, O., Geroldi, C., 2002 Oct. Mild cognitive impairment with subcortical vascular features: clinical characteristics and outcome. J. Neurol. 249 (10), 1423–1432.

Giorgio, A., Battaglini, M., Rocca, M.A., et al., 2013 Jan 15. Location of brain lesions predicts conversion of clinically isolated syndromes to multiple sclerosis. Neurology 80 (3), 234–241.

Hagens, M.H.J., Burggraaff, J., Kilsdonk, I.D., et al., 2018 Jul 17a. Three-tesla MRI does not improve the diagnosis of multiple sclerosis: a multicenter study. Neurology 91 (3), e249–e257.

Hagens, M.H., Burggraaff, J., Kilsdonk, I.D., et al., 2018b. Impact of 3 Tesla MRI on interobserver agreement in clinically isolated syndrome: a MAGNIMS multicentre study. Multiple Sclerosis (Houndmills, Basingstoke, England) 25 (3), 352–360 (Jan 1:1352458517751647)3.

Jenkinson, M., Smith, S., 2001 Jun. A global optimisation method for robust affine registration of brain images. Med. Image Anal. 5 (2), 143–156.

Jenkinson, M., Beckmann, C.F., Behrens, T.E., Woolrich, M.W., Smith, S.M., 2012 Aug 15. Fsl. NeuroImage 62 (2), 782–790.

Karnath, H.O., Sperber, C., Rorden, C., 2018 Jan 15. Mapping human brain lesions and their functional consequences. NeuroImage 165, 180–189.

Kuo, H.K., Lipsitz, L.A., 2004 Aug. Cerebral white matter changes and geriatric syndromes: is there a link? J. Gerontol. A Biol. Sci. Med. Sci. 59 (8), 818–826.

Maillard, P., Fletcher, E., Harvey, D., et al., 2011 Jul. White matter hyperintensity penumbra. Stroke 42 (7), 1917–1922.

Mascalchi, M., Salvadori, E., Toschi, N., et al., 2018. DTI-derived indexes of brain WM correlate with cognitive performance in vascular MCI and small-vessel disease. A TBSS study. Brain Imaging Behav (Epub ahead of print).

Matthews, L., Marasco, R., Jenkinson, M., et al., 2013 Apr 2. Distinction of seropositive NMO spectrum disorder and MS brain lesion distribution. Neurology 80 (14), 1330–1337.

Narayanan, S., Fu, L., Pioro, E., et al., 1997 Mar. Imaging of axonal damage in multiple sclerosis: spatial distribution of magnetic resonance imaging lesions. Ann. Neurol. 41 (3), 385–391.

O'Brien, J.T., Erkinjuntti, T., Reisberg, B., et al., 2003 Feb. Vascular cognitive impairment. Lancet Neurol. 2 (2), 89–98.

O'Sullivan, M., Jones, D.K., Summers, P.E., Morris, R.G., Williams, S.C., Markus, H.S., 2001 Aug 28. Evidence for cortical "disconnection" as a mechanism of age-related cognitive decline. Neurology 57 (4), 632–638.

Pantoni, L., 2010 Jul. Cerebral small vessel disease: from pathogenesis and clinical characteristics to therapeutic challenges. Lancet Neurol. 9 (7), 689–701.

Pantoni, L., Basile, A.M., Pracucci, G., et al., 2005. Impact of age-related cerebral white matter changes on the transition to disability – the LADIS study: rationale, design and methodology. Neuroepidemiology 24 (1–2), 51–62.

Pantoni, L., Poggesi, A., Inzitari, D., 2007 Aug. The relation between white-matter lesions and cognition. Curr. Opin. Neurol. 20 (4), 390–397.

Poggesi, A., Salvadori, E., Pantoni, L., et al., 2012. Risk and determinants of dementia in patients with mild cognitive impairment and brain subcortical vascular changes: a study of clinical, neuroimaging, and biological markers-the VMCI-Tuscany study: rationale, design, and methodology. Int. J. Alzheimers Dis. 2012, 608013.

Salvadori, E., Poggesi, A., Pracucci, G., Inzitari, D., Pantoni, L., 2015. Development and psychometric properties of a neuropsychological battery for mild cognitive impairment with small vessel disease: the VMCI-Tuscany Study. J. Alzheimers Dis. 43 (4), 1313–1323.

Salvadori, E., Poggesi, A., Valenti, R., et al., 2016 Apr. Operationalizing mild cognitive impairment criteria in small vessel disease: the VMCI-Tuscany Study. Alzheimers Dement. 12 (4), 407–418.

Seo, S.W., Ahn, J., Yoon, U., et al., 2010 Jan. Cortical thinning in vascular mild cognitive impairment and vascular dementia of subcortical type. J. Neuroimaging 20 (1), 37–45.

Smith, S.M., Nichols, T.E., 2009 Jan 1. Threshold-free cluster enhancement: addressing problems of smoothing, threshold dependence and localisation in cluster inference. NeuroImage 44 (1), 83–98.

Smith, S.M., Zhang, Y., Jenkinson, M., et al., 2002 Sep. Accurate, robust, and automated longitudinal and cross-sectional brain change analysis. NeuroImage 17 (1), 479–489.

Smith, S.M., Jenkinson, M., Woolrich, M.W., et al., 2004. Advances in functional and structural MR image analysis and implementation as FSL. NeuroImage 23 (Suppl. 1), S208–S219.

Vik, A., Hodneland, E., Haasz, J., Ystad, M., Lundervold, A.J., Lundervold, A., 2015. Fractional anisotropy shows differential reduction in frontal-subcortical fiber bundles-a longitudinal MRI study of 76 middle-aged and older adults. Front. Aging Neurosci. 7, 81.

Wardlaw, J.M., Valdes Hernandez, M.C., Munoz-Maniega, S., 2015 Jun 23. What are white matter hyperintensities made of? Relevance to vascular cognitive impairment. J. Am. Heart Assoc. 4 (6), 001140.

Wen, W., Sachdev, P., 2004 May. The topography of white matter hyperintensities on brain MRI in healthy 60- to 64-year-old individuals. NeuroImage 22 (1), 144–154.

Winblad, B., Palmer, K., Kivipelto, M., et al., 2004 Sep. Mild cognitive impairment–beyond controversies, towards a consensus: report of the International Working Group on Mild Cognitive Impairment. J. Intern. Med. 256 (3), 240–246.